Ion Channels in Yeast

MICHAEL C. GUSTIN, BORIS MARTINAC, YOSHIRO SAIMI, MICHAEL R. CULBERTSON, CHING KUNG

Voltage-dependent ion channels have been found in the plasma membrane of the yeast *Saccharomyces cerevisiae*. Ion channel activities were recorded from spheroplasts or patches of plasma membrane with the patch-clamp technique. The most prominent activities came from a set of potassium channels with the properties of activation by positive but not negative voltages, high selectivity for potassium over sodium ion, unit conductance of 20 picosiemens, inhibition by tetraethylammonium or barium ions, and bursting kinetics.

ION CHANNELS ARE FOUND IN A WIDE variety of tissues and organisms in both plants and animals. Ion channels are a class of proteins that function as gated pores in the cell membrane, allowing the flow of ions down electrical or chemical gradients. However, genetic dissection of ion channel function has been carried out in *Paramecium* (*1*) and *Drosophila* (*2*). Among eukaryotes, the yeast *Saccharomyces cerevisiae* can be manipulated genetically most easily (*3*). A genetic approach, coupled with the ability to record ion-channel activities in the plasma membrane of yeast, would serve to advance our knowledge of channel structure, function, and regulation. Toward this goal, we have begun to study the ion channels in the plasma membrane of yeast spheroplasts with the patch-clamp technique (*4*).

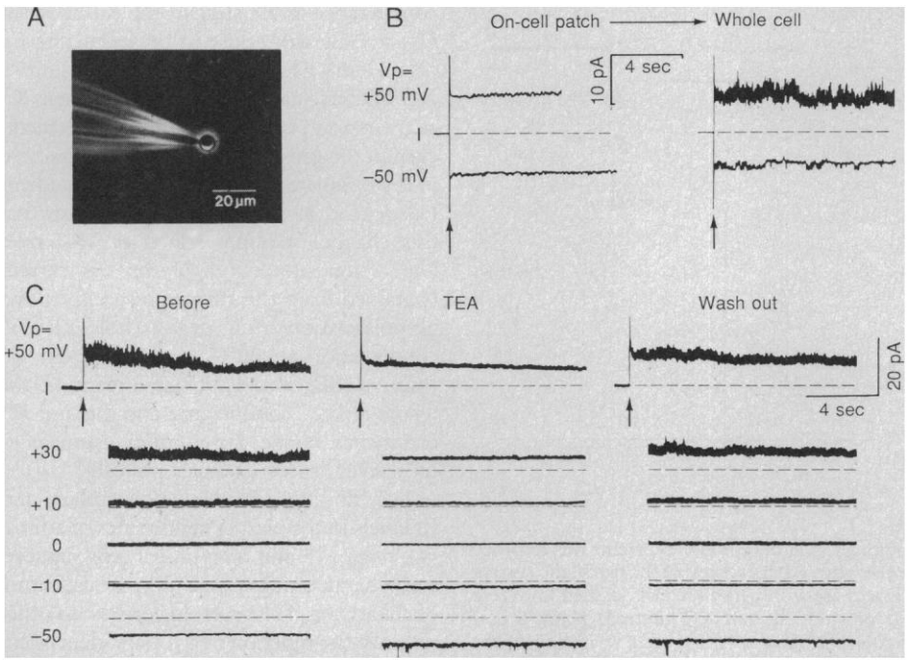

Fig. 1. Whole-cell currents from spheroplasts. (A) Phase-contrast micrograph of a spheroplast on a patch-clamp pipette. (B) Establishing the whole-cell mode. (Left) Currents from an on-cell patch. The electrode formed a 6-gigaohm seal on a spheroplast and the application of +50 mV (positive pipette voltage, V_p; arrows indicate onset of voltages from 0 mV) yielded a seal current of about 8 pA out of the pipette (upper trace, left; broken line indicates the zero-current level). (Right) Currents from the whole-cell mode recorded from the same spheroplast as left. Transition to this recording mode from the on-cell patch was characterized by the presence of a prominent, rapidly fluctuating current (+50 mV, upper trace, right). This current was absent at −50 mV (lower trace, right). The seal current decreased slightly in this case as the seal improved upon the additional suction applied to establish the whole-cell mode. Solutions used were 100 m*M* KCl (pipette); 50 m*M* KCl, 50 m*M* NaCl, 20 m*M* $MgCl_2$ (bath) at 20°C. In Fig. 1, B and C, and Fig. 2, A to C, pipette solutions contained additionally 3 m*M* $CaCl_2$, 0.1 m*M* Na_2EDTA, and 5 m*M* Hepes-KOH (*p*H 7.2); bath solutions contained additionally 1 m*M* EGTA, 0.98 m*M* $CaCl_2$ (10^{-5} *M* free Ca^{2+}), and 5 m*M* Hepes-KOH (*p*H 7.2); these components add an additional 2 m*M* K^+ to all solutions. (C) Families of whole-cell currents from a different spheroplast at the pipette voltages (V_p) marked on the left. (Left) The fluctuating current is only observed at positive voltages. Upon a strong and prolonged depolarization (such as +50 mV), the current slowly relaxed. Arrows indicate onset of voltage from 0 mV; dashed lines indicate the zero-current level. (Middle) The prominent asymmetric current was suppressed by 20 m*M* TEA and recovered (right) when the TEA was washed out. All currents shown were filtered at 1 kHz and replayed on a chart recorder. The solutions used were 150 m*M* KCl (pipette); 50 m*M* KCl, 100 m*M* NaCl, 50 m*M* $MgCl_2$, ±20 m*M* TEA-Cl (bath); 20°C.

Spheroplasts of diploid yeast were prepared with Zymolyase (*5*) to remove the cell wall. Gigaohm seals were formed between patch pipettes (5 to 10 megohms) and larger spheroplasts, averaging 7 to 10 μm in diameter. Seal resistances ranged between 1 to 40 gigaohms, usually about 4 gigaohms. Requirements for gigaohm seal formation were (i) millimolar concentrations of Mg^{2+} or Ca^{2+} in the bath and pipette solutions and (ii) vigorous suction of the spheroplast onto the pipette. Formation of the gigaohm seal was generally slow (tens of seconds).

Once a gigaohm seal formed on the intact cell, a whole-cell recording mode was achieved by applying additional suction or large voltage pulses. There were two consequences of this transition. (i) Under phase-contrast optics, the cell interior became darker, possibly because of an exchange of cytoplasmic constituents with the pipette solution. (ii) A depolarization-activated current was observed. The currents responding to voltage steps of +50 or −50 mV (V_p) are shown (Fig. 1B) for both the on-cell patch mode (left) and the whole-cell mode (right), recorded from the same spheroplast. Note that in the whole-cell mode, a positive pipette voltage (V_p) is a depolarizing voltage for the cell membrane. An outward current was seen in the whole-cell mode only upon depolarization and not upon hyperpolarization. This asymmetric current is diagnostic of the whole-cell recording that has been achieved over a hundred times. Although hyperpolarization-activated currents were also observed in the whole-cell mode, these were generally unstable and thus difficult to study.

Because of its prominence and stability, the depolarization-activated current was analyzed in greater detail both in the whole-cell recording mode (Fig. 1, B and C, and Fig. 2B) and in excised outside-out patches (Fig. 2A). The relation between this membrane current and applied voltage is shown in Fig. 1C. Above a threshold of −10 to 0 mV, increasing voltage resulted in larger and larger currents that fluctuated rapidly over a range of approximately 10 pA upon depolarization to +50 mV. The fluctuation probably resulted from a summation of many rapidly gating channels of unit conductance (see below). When large depolarizing voltages were sustained, the activated

Laboratory of Molecular Biology and the Department of Genetics, University of Wisconsin–Madison, Madison, WI 53706.

current relaxed over time (Fig. 1C, upper left). Addition of 20 m*M* tetraethylammonium chloride (TEA-Cl) to the bath solution reversibly inhibited the depolarization-activated current (Fig. 1C). Addition of 10 m*M* $BaCl_2$ to the bath also inhibited the depolarization-activated current, while 10 m*M* tetramethylammonium chloride or 10 m*M* $CaCl_2$ was without effect. Since TEA^+ and Ba^{2+} block K^+ channels in many systems (*6*), these results suggest that the depolarization-activated current is carried by K^+. Varying the free Ca^{2+} concentration between $10^{-7}M$ and $10^{-2}M$ in the pipette had no effect on the depolarization-activated current, suggesting that this K^+ conductance is not regulated by intracellular Ca^{2+}.

Two approaches were used to examine the unitary conductance activated by positive voltages. One procedure was to excise outside-out patches starting from the whole-cell recording mode (Fig. 2A). In such excised patches, the depolarization-activated current was smaller than in the whole cell and showed bursting behavior. A second procedure was to hold the voltage in the whole-cell mode at +40 mV or greater. With sustained depolarization the current relaxed from an initial peak value to a new steady state (Fig. 2B, upper trace). Periods in which all of the depolarization-activated current was inactivated (arrow) alternated with periods in which one or sometimes more equal step increases in current were observed (arrowhead). Such quantum levels of current were observed only upon depolarization and were blocked by external 20 m*M* TEA-Cl. When these bursts of unitary current were examined at better frequency resolution (Fig. 2B, lower trace), we observed clear transitions of picoampere current between two levels (closed and open), characteristic of a channel-type conductance mechanism (*7*).

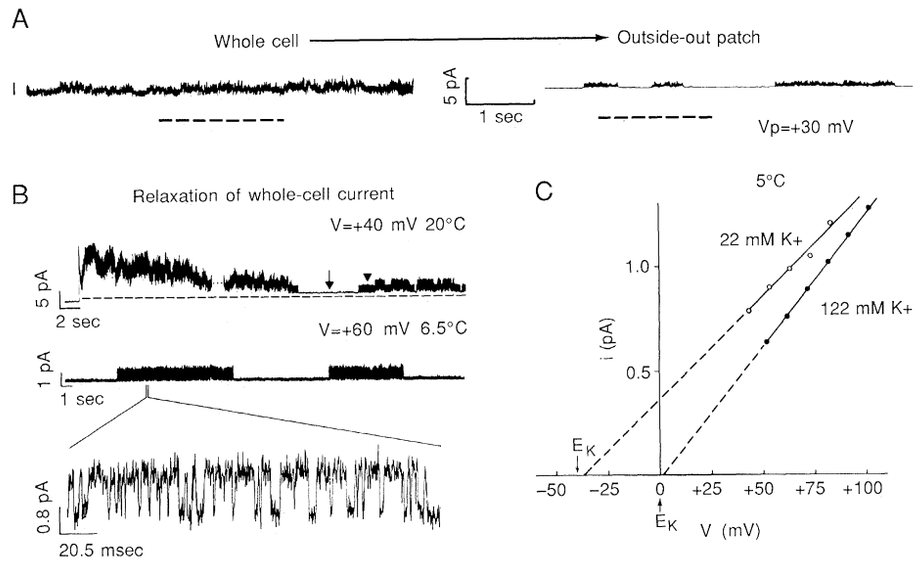

Fig. 2. Single-channel currents. (A) The unitary current underlying the ensemble currents was recorded from an outside-out patch (right) excised from a whole cell (left). After excision of the patch, the current was greatly reduced and showed bursting behavior. Traces are from chart records (dashed line, zero current level). The solutions used were 100 m*M* KCl (pipette); 50 m*M* KCl, 50 m*M* NaCl, 5 m*M* $MgCl_2$ (bath); 20°C. (B) (Upper trace) Unitary currents were also recorded after relaxation of the whole-cell ensemble currents. A voltage step from −40 to +40 mV caused a relaxation of the whole-cell ensemble over tens of seconds (dots) to a new steady state where all channels were closed some of the time (arrow), followed by bursts of activities from one or more channels (arrowhead). Data from chart record. The solutions were 180 m*M* KCl (pipette); 30 m*M* KCl, 150 m*M* NaCl, 5 m*M* $MgCl_2$ (bath); 20°C. (Middle and lower trace) Single-channel bursts after ensemble relaxation, examined at higher time resolution, revealed clear open and close states characteristic of ion-channel behavior. (Middle trace) Data from chart record; (lower trace) the computer display from the same recording stored on magnetic tape and fed into an INDEC $11–23^+$ computer with a 0.1-msec sampling rate after filtration at 2 kHz (8-pole Bessel filter). The solutions for the middle and lower traces were 150 m*M* KCl (pipette); 30 m*M* KCl, 120 m*M* NaCl, 50 m*M* $MgCl_2$ (bath); 6.5°C. (C) Current-voltage relationship of unitary current. Flat-top unitary currents were taken from a recording in whole-cell mode after ensemble current relaxation [see legend to (B)]. Inspection of recorded data was the same as for (B). Lower trace (see above) except that filtration was at 1 kHz. Pipette solution was 120 m*M* KCl. Bath solution was initially 120 m*M* KCl, 40 m*M* $MgCl_2$, and 5 m*M* $CaCl_2$ (●) and, after perfusion, 20 m*M* KCl, 100 m*M* NaCl, 40 m*M* $MgCl_2$ and 5 m*M* $CaCl_2$ (○), both at 5°C. Calculated K^+ equilibrium potentials (arrows) were 0 mV and −41 mV, respectively. Only data for the minimum conductance state of the channel are plotted. A second, higher conductance state of the channel was also observed at 5°C. The ratio of the two slope conductances was 1.3 ± 0.1 (mean ± SD, $n = 5$). This ratio appeared to be independent of the ion composition of the bath. Changing K^+ concentration in the bath produced shifts in the extrapolated E_{rev} for the two conductance states that were the same as the shifts in calculated E_K. Since the minimum conductance state was most frequently encountered, only data concerning this state are shown.

By use of single-channel recordings from both excised patches and whole-cell mode, we determined the slope conductance for the depolarization-activated current (2 kHz filtered) to be 20.5 ± 3.9 pS (mean ± SD, $n = 7$) at 20°C. Only flat-topped current transitions were analyzed. However, because of the characteristic rapid flickering of channel open-close events at 20°C, we also measured slope conductance at 5°C. With 122 m*M* K^+ in both pipette and bath, the slope conductance for the minimum conductance state (see legend to Fig. 2C) of the depolarization-activated current was 13 pS (Fig. 2C). The extrapolated reversal potential (E_{rev}) of 2 mV for this current was close to the expected K^+ equilibrium potential (E_K) of 0 mV. Replacement of 100 m*M* K^+ in the bath solution with 100 m*M* Na^+ resulted in a small reduction in the slope conductance and a shift in the extrapolated E_{rev} to −37 mV, close to the calculated E_K of −41 mV (Fig. 2C). The parallel shift of E_{rev} and calculated E_K further indicates K^+ as the major permeant ion. This agreement, even in the presence of a large Na^+ gradient in the opposite direction of the K^+ gradient (see legend to Fig. 2C), also indicates that this channel strongly selects for K^+ over Na^+. After subtraction of the seal current (obtained from the current response to hyperpolarization) the peak whole-cell K^+ conductance at 20°C was 151 ± 20 pS (mean ± SD, $n = 4$). Comparisons of the whole-cell K^+ conductance and the unit K^+ conductance give a minimum estimate of only seven to ten channels per cell.

The finding of voltage-dependent ion channels in the plasma membranes of animal (*4*), plant (*8*), and now fungal cells suggests such channels might be a ubiquitous feature of eukaryotes. However, in contrast to other systems, the function of a voltage-dependent K^+ channel in yeast is unclear. Fungi use a proton electrochemical potential ($\Delta\bar{\mu}_{H^+}$) (*9*), primarily generated by an adenosine triphosphate–driven H^+ extrusion pump in the plasma membrane (*10*), to facilitate uptake of nutrients (*11*). The membrane potential (interior negative) of the cell is one component of $\Delta\mu_{H^+}$. Perhaps voltage-dependent K^+ channels play a role in the homeostatic regulation of the cell membrane potential.

The successful recording of single-channel activity in the yeast plasma membrane creates several opportunities. The genetic advantages of yeast can be exploited to study the structure, function, assembly, and regulation of native channels through mutant selection and analysis. Foreign channel

genes introduced by transformation (*12, 13*) into yeast may be expressed and channel activity recorded. The effect of site-specific mutagenesis of the channel gene (*14*) on channel function could then be analyzed.

REFERENCES AND NOTES

1. C. Kung and Y. Saimi, *Curr. Top. Membr. Transp.* **23**, 45 (1985).
2. J. C. Hall, in *Comprehensive Insect Physiology, Biochemistry and Pharmacology*, G. A. Kerkut and L. I. Gilbert, Eds. (Pergamon, Oxford, 1983), vol. 9.
3. H. Roman, in *The Molecular Biology of the Yeast Saccharomyces, Life Cycle and Inheritance*, J. N. Strathern, E. W. Jones, J. R. Broach, Eds. (Cold Spring Harbor Press, Cold Spring Harbor, NY, 1982), p. 1.
4. O. P. Hamill, A. Marty, E. Neher, B. Sakmann, F. J. Sigworth, *Pfluegers Arch. Gesamte Physiol.* **391**, 85 (1981).
5. K. Kitamura and Y. Yamamoto, *Arch. Biochem. Biophys.* **153**, 403 (1972).
6. R. Latorre and C. Miller, *J. Membr. Biol.* **71**, 11 (1983); C. Vergara and R. Latorre, *J. Gen. Physiol.* **82**, 543 (1983).
7. B. Hille, *Ionic Channels of Excitable Membranes* (Sinauer, Sunderland, MA, 1984), p. 201.
8. J. I. Schroeder, R. Hedrich, J. M. Fernandez, *Nature (London)* **312**, 361 (1984); N. Moran *et al.*, *Science* **226**, 835 (1984).
9. C. L. Slayman, *J. Gen. Physiol.* **49**, 93 (1965); D. Sanders, U.-P. Hansen, C. L. Slayman, *Proc. Natl. Acad. Sci. U.S.A.* **78**, 5903 (1981); P. De La Peña *et al.*, *Eur. J. Biochem.* **123**, 447 (1982).
10. F. Malpartida and R. Serrano, *J. Biol. Chem.* **256**, 4175 (1981); A. Goffeau and C. W. Slayman, *Biochim. Biophys. Acta* **639**, 197 (1981); D. S. Perlin *et al.*, *J. Biol. Chem.* **59**, 7884 (1984).
11. A. A. Eddy and J. A. Nowacki, *Biochem. J.* **120**, 845 (1971).
12. A. Hinnen, J. B. Hicks, G. R. Fink, *Proc. Natl. Acad. Sci. U.S.A.* **75**, 1929 (1978); J. D. Beggs, *Nature (London)* **275**, 104 (1978).
13. N. Fujita, N. Nelson, T. D. Fox, T. Claudio, G. P. Hess, *Science* **231**, 1284 (1986).
14. M. J. Zoller and M. Smith, *Methods Enzymol.* **100**, 468 (1983).

15. We thank R. Ramanathan, R. Hinrichsen, and A. Burgess-Cassler for helpful comments on the manuscript, C. Smith for technical assistance, and S. Limbach for photographic assistance. Supported by NIH (GM-22714 to C.K. and GM-26217 to M.C.) and NSF (BNS-8216149 to C.K. and Y.S.) grants.

3 March 1986; accepted 16 June 1986

Altered K^+ Channel Expression in Abnormal T Lymphocytes from Mice with the *lpr* Gene Mutation

K. GEORGE CHANDY, THOMAS E. DECOURSEY, MICHAEL FISCHBACH, NORMAN TALAL, MICHAEL D. CAHALAN, SUDHIR GUPTA

The observation that voltage-dependent K^+ channels are required for activation of human T lymphocytes suggests that pathological conditions involving abnormal mitogen responses might be reflected in ion channel abnormalities. Gigaohm seal techniques were used to study T cells from MRL/MpJ–*lpr*/*lpr* mice; these mice develop generalized lymphoproliferation of functionally and phenotypically abnormal T cells and a disease resembling human systemic lupus erythematosus. The number and predominant type of K^+ channels in T cells from these mice differ dramatically from those in T cells from control strains and a congenic strain lacking the *lpr* gene locus. Thus an abnormal pattern of ion channel expression has now been associated with a genetic defect in cells of the immune system.

RECENT STUDIES WITH THE GIgaohm seal technique indicate that the most abundant ion channel in human and murine T lymphocytes is a voltage-gated K^+ channel closely resembling the delayed rectifier of muscle and nerve (*1–5*). Sodium channels have been detected only infrequently in T lymphocytes, and calcium channels have not been observed thus far. Several types of evidence suggest that K^+ channels play a necessary role during human T-lymphocyte activation and proliferation (*1, 4, 6*). In this report we show that K^+ channels in murine T cells play a similar role. In addition, we have taken advantage of the existence of a strain of mice, MRL/MpJ–*lpr*/*lpr* (MRL-l), with genetically induced abnormalities of T lymphocytes (*7*), to further explore the involvement of K^+ channels in T-cell proliferation.

MRL-l mice that are homozygous for the autosomal recessive *lpr* mutation, develop severe lymph node enlargement early in life that reflects polyclonal expansion of a T-cell subset with a unique set of cell surface markers (*8*). The abnormal subset of T cells does not actively cycle in vivo, and may represent cells arrested at an immature stage of differentiation (*9*). These cells display impaired interleukin-2 production and proliferation in response to mitogens in vitro (*7, 10*). The congenic control strain, MRL/MpJ–+/+ (MRL-n), which differs from MRL-l mice only in lacking the *lpr* mutation, does not develop lymphoproliferation, and T lymphocytes from these mice express a normal phenotype and respond normally to mitogens in vitro (*7–10*). In addition, they exhibit a lupus-like disease much later in life than MRL-l mice (*7*). Thus, young congenic MRL-n mice represent a useful control for comparative studies.

Figure 1 shows outward K^+ currents recorded from individual MRL-l and MRL-n T lymphocytes. Superficially, these K^+ currents resemble those in human T lymphocytes (*3*). MRL-n T cells typically had on the order of ten K^+ channels per cell, with a low average (±SEM) maximum K^+ conductance, g_K, of 0.37 ± 0.10 nS ($n = 38$). The g_K of 26 T cells from four other control mouse strains (CBA/J, C57BL/6J, BALB/c, and C3H/HeJ) that do not spontaneously develop lymphadenopathy or autoimmune manifestations ranged from 0.01 to 0.54 nS (*5*). The g_K was similar in T lymphocytes from lymph node and spleen among the five control strains; therefore these results have been pooled. K^+ currents in T cells from MRL-l mice were substantially larger than in the control strains. The average ± SEM g_K for all the MRL-l T lymphocytes was 4.6 ± 0.6 nS ($n = 31$). T cells from MRL-l lymph nodes ($n = 23$) had uniformly high g_K values. The g_K in MRL-l splenic T cells was more variable, with two of eight cells having low g_K values in the range for T cells from normal mice, probably reflecting normal T cells in the population. The spleens from MRL-l mice have a lower fraction of cells with the aberrant phenotype (*8, 11*). In one experiment, the fraction of phenotypically abnormal splenic T cells was enriched by selecting for Lyt-1^+2^- T cells (*11*). The three purified MRL-l splenic T cells studied had a consistently high g_K, comparable to that in lymph node MRL-l T cells. In contrast, two purified Lyt-1^+2^- T cells from control MRL-n mice had very low g_K values, in the range for normal mouse T cells. Dividing the g_K by the measured single K^+ channel conductance gave an estimate of 220 K^+ channels in a typical MRL-l T lymphocyte and about 12 K^+ channels per MRL-n T lymphocyte. Thus, T cells from diseased MRL-l mice have more than an order of magnitude more K^+ channels than normal mouse T lymphocytes. With the exception of Na^+ channels sometimes ob-

K. G. Chandy and S. Gupta, Division of Basic and Clinical Immunology, Department of Medicine, University of California, Irvine, CA 92717.
T. E. DeCoursey, Department of Physiology, Rush-Presbyterian-St. Luke's Medical Center, Chicago, IL 60612.
M. Fischbach and N. Talal, Department of Medicine, Audie Murphy Veterans Administration Hospital, University of Texas Health Sciences Center, San Antonio, TX 78284.
M. D. Cahalan, Department of Physiology and Biophysics, University of California, Irvine, CA 92717.